Titanian aegirine in a teschenite sill

D. J. MARTIN

School of Earth Sciences, Macquarie University, Sydney, Australia

ABSTRACT. A miscibility gap exists between titansahlite and late-stage titanian aegirine in a teschenitic sill, with coexisting kaersutite plotting between them. A second series of titansahlite–sodian-ferrosahlite–aegirine-augite is continuous.

TWO series of pyroxenes have been found in a layered teschenite sill, 22 m thick, emplaced in Late Permian coal measures in the Sydney Basin, New South Wales, Australia. The sill consists of 12 m of homogeneous teschenite, overlain by 6 m of picrite, then by 4 m of a layered sequence. The layering unit of this sequence is teschenite, a pyroxene-rich layer and a narrow leucocratic band. A whole-rock analysis of the lower chilled margin (Table I, anal. 1) gives (Na + K)/Al of 0.68, and one of the layers containing aegirine (Table I, anal. 2) a ratio of 0.72, indicating that the magma is not peralkaline. The presence in the sill of spinel lherzolite microxeno-liths and olivine megacrysts (Fo_{90}), with a whole-rock Mg number [$100Mg/(Mg+Fe^{2+})$] of 71, evidences the primitive nature of the magma (Frey et al., 1978).

Occurrence of the pyroxenes. The most common pyroxene throughout the sill is a pink, sector-zoned titansahlite (Table I, anal. 3). In the pyroxene-rich layers this is accompanied by calcic labradorite, titanomagnetite, titanian biotite, rare olivine, apatite and interstitial sanidine (now largely analcitised). Ti-rich amphibole, kaersutite, may rim titansahlite grains, or occur as stubby euhedra. Some titansahlite grains, commonly near the leucocratic bands, are rimmed by pale green sodian ferrosahlite (Table I, anal. 4).

Long prismatic grains of kaersutite are the principal mafic phase, with minor biotite and titanomagnetite, in the labradorite-rich leucocratic bands. Small grains of deep green aegirine-augite (Table I, anal. 5) are nucleated on the amphibole, and also occur in small clusters among the sanidine grains of the pyroxene-rich layers.

The widest pyroxene-rich layer (1 m thick) contains numerous cavities, and has the most Ti-enriched biotite, the lowest Nb/Zr ratio of this layer-type, and the highest Rb/Sr ratio of the whole sill.

These characters suggest it is the most evolved layer of the sequence. The cavities, in clots of titansahlite, are filled with Na zeolites and analcite. They are lined with terminated pyroxene prisms, zoned from basal titansahlite, through neutral to deep blue-green tips of titanian aegirine (Table I, anal. 7). These phases are optically continuous.

Pyroxene geochemistry. All compositions were determined on a wavelength-dispersive ETEC Autoprobe, with an acceleration voltage of 15 kV, and a 50 na specimen current. Minimum beam diameter used was 10 nm, and grain boundaries were checked with a scanning electron microscope. Following the suggestion of Ferguson (1978), the pyroxenes of single samples have been plotted separately on a $Na–Mg–Fe^{2+}$ diagram (fig. 1a). The coexisting kaersutite has been normalized to the same Fe^{3+}/Fe^{2+} ratio as a kaersutite from the Iki Islands, Japan (Aoki, 1959).

The pyroxenes from 19 m above the base of the intrusion have an *mg* number [$100 Mg/(Mg + total Fe)$] of 81 to 87 in the titansahlites, and of 50 to 9.6 in the titanian aegirines. Maximum Na and Fe enrichment occur together (Table I, anal. 6), with a ratio of Fe^{3+}/Fe^{2+} of 12.7 (calculated stoichiometrically). A marked compositional gap occurs between the Ca-rich and the Na-rich pyroxenes. Kaersutite coexists in the layer, although not in the cavities, and plots in this region of pyroxene instability.

A series of pyroxenes from the next lower pyroxene-rich layer (18.6 m above base) is shown for comparison. The *mg* number varies from 71 to 67 in titansahlite, and from 66 to 31 in sodian Fe-rich compositions. No region of pyroxene instability is present, and variation from titan-sahlite to sodian ferrosahlite to aegirine-augite is continuous. However, the coexisting amphibole occupies a position similar to the amphibole of the more sodic series. A Na–Ti–total-Fe diagram (fig. 1b) confirms that the Na–Fe pyroxenes of the two series do not overlap, and show continuous solid solution between titansahlite and aegirine-augite. On a $Na–Ti–Fe^{3+}$ plot (fig. 1c) the titanian aegirine analyses form a tight group.

TABLE I.   Analyses of some rocks and minerals from Scone, N.S.W.

	1	2	3	4	5	6	7
SiO_2	45.5	48.2	50.0	49.8	48.9	51.6	52.1
TiO_2	2.74	2.62	1.45	0.82	1.33	0.67	3.82
Al_2O_3	13.9	15.7	2.99	2.0	1.23	1.03	0.15
Fe_2O_3	3.05	4.39	3.12	4.22	6.65	3.46	23.3
FeO	8.22	5.31	5.54	11.8	13.6	6.09	2.86
MnO	0.18	0.14	0.23	0.35	0.62	0.21	0.20
MgO	11.2	5.68	13.5	7.9	5.8	13.1	1.19
CaO	8.22	9.84	22.8	22.2	19.7	22.7	3.36
Na_2O	4.27	4.86	0.41	1.18	2.19	0.77	11.8
K_2O	2.24	3.12	-	-	-	-	-
P_2O_5	0.6	0.66	-	-	-	-	-
Total	100.1	100.1	100.1	100.2	99.5	99.82	99.5
L.o.I.	3.31	4.58					
mg	65	51	74	47	75	79	12

1. Whole-rock analysis, lower chilled margin of teschenite, 0.86 m.
2. Whole-rock analysis, pyroxene-rich layer, 19.04 m.
3. Pink titansahlite, 19.08 m.
4. Sodian ferrosahlite, green rim on titansahlite, 18.6 m.
5. Aegirine-augite, deep green grain, 18.6 m.
6. Neutral base of grain in cavity, 19.08 m.
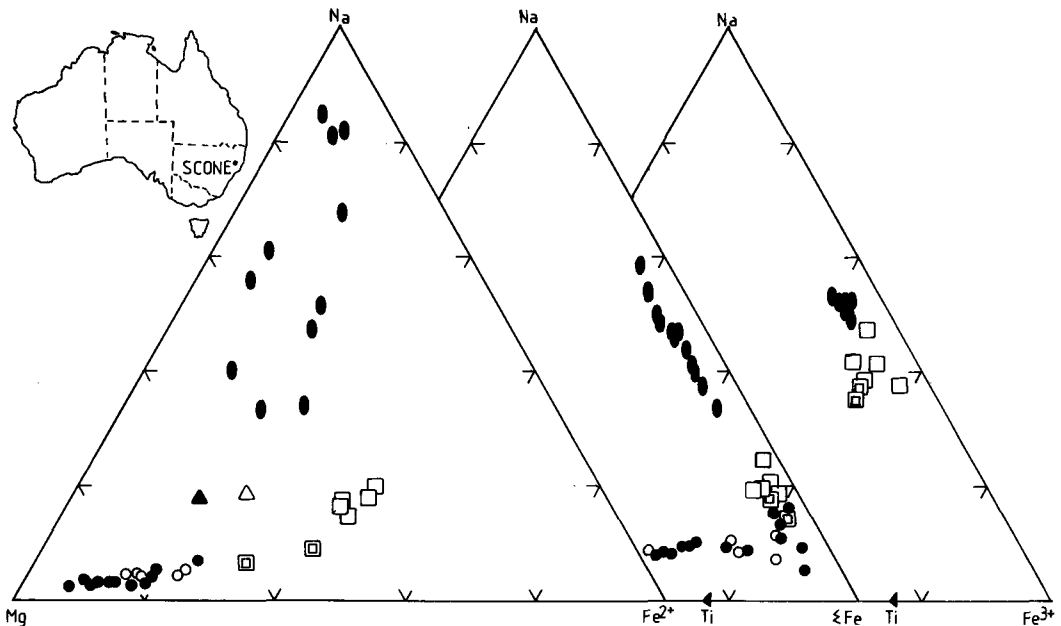7. Titanian aegirine, tip of grain, analysis 6, 19.08 m.

FIG. 1. Pyroxenes and amphiboles of two evolved leucocratic bands in the Scone teschenite. Circles, titansahlite; ovals, titanian aegirine; double squares, ferrosahlite; squares, aegirine-augite; triangles, kaersutite. Filled symbols, band at 19 m; other symbols, band at 18.6 m. (a) The alkali pyroxene triangle $Mg-Fe^{2+}-Na$; (b) Ti–total-Fe–Na; (c) $Ti-Fe^{3+}-Na$.

Discussion. Significant amounts of Ti have been found in aegirine occurring as late-stage pyroxene in peralkaline rocks, such as the Las Canadas lavas, Tenerife (Scott, 1976), welded ignimbrites of Gran Canaria (Flower, 1974), Danish peralkaline ash layers (Pedersen *et al.*, 1975; Rønsbo *et al.*, 1977) and in ultramafic complexes in Greenland (Larsen, 1976). Ferguson (1977*a, b*) reports titanian aegirine lining vesicles in volcanic rocks with peralkaline affinities, including Eastern Australian leucitite, quartz syenite, quartz-bearing alkali trachyte and nephelenite. Aegirine from a teschenitic intrusion of the Morotu District, Sakhalin (Yagi, 1953, Table 6, anal. 1411) is described as bluish green, contains 2.34 wt. % TiO_2, and may be close to titanian aegirine in composition. However, the silica content is more characteristic of aegirine-augite.

The aegirine in the Scone sill is not so Ti-rich as some of those analysed by Ferguson (1977*a*), but resembles that found in a phonolite from Bohemia (Table I, anal. 7 of Ferguson, 1977*a*). The presence of aegirine implies the formation of Na silicate in the magma, i.e. the development of peralkalinity (Bailey and Schairer, 1966). Although this is commonly caused by depletion of Al by feldspar fractionation (Bailey, 1969) this does not seem to have occurred in the teschenite, since the cavity fills are natrolite and analcime. Extreme Na enrichment of the residual liquid was more probably due to Ca depletion by extensive local crystallization of sahlite with low Na content.

The varying Na/total Fe ratio (fig. 1*b*) may represent solid solution between aegirine $NaFe^{3+}Si_2O_6$, and neptunite, $Na_2(Mg,Fe^{2+})Ti(Si_2O_6)_2$ (Ferguson, 1977*a*). On Na–Ti–Fe^{3+} axes (fig. 1*c*) the clustering of the aegirine analyses suggests that the spread in figs. 1*a* and *b* is due to $Mg \rightleftharpoons Fe^{2+}$ substitution in the neptunite, rather than a change in the proportion of aegirine. Formation of Mg-rich neptunite is favoured by higher oxygen fugacity (Nielsen, 1979), while Fe-rich neptunite results from local lowering of oxygen fugacity. A high oxygen fugacity in the teschenite magma is inferred from the extreme scarcity of ilmenite, and partitioning of Ti into silicates (Haggerty, 1976). The presence of F in the kaersutite, of CO_2 (evidenced by primary calcite in cavity fills) and H_2O (inferred from the abundance of hydrated minerals) suggests a high volatile partial pressure, which would stabilize amphibole to a high temperature (Ernst, 1968).

Fe–Ti oxide pairs, where available, indicate that they equilibrated at about 1150 °C, and an oxygen fugacity on the QFM buffer. Nielsen (1979) concluded that aegirine formed at near-liquidus temperature and fairly high oxygen fugacity. The

residual fluid in the cavities must have been still more volatile-rich; such conditions would increase the activity of Fe^{3+} relative to that of Fe^{2+} (Kogarko and Krigman, 1973), and favour the formation of aegirine.

Textural evidence shows that aegirine-augite formed after kaersutite in the less Na-rich series. No pyroxene gap is present. Calcic amphibole takes a role similar to that of the alkali amphibole commonly present in peralkaline rocks.

Conclusions. The occurrence of titanian aegirine in teschenite confirms Ferguson's (1977*a*) conclusion that aegirine can form if peralkalinity is attained, irrespective of silica activity of the original magma. The presence of a pyroxene gap between coexisting Ca-rich and Na-rich pyroxene can be detected when the pyroxenes of a single sample are plotted, more easily than when data from a suite are combined on a single diagram. A high Ti and volatile content appear to contribute to the presence of a miscibility gap.

REFERENCES

Aoki, K. (1959) *Sci. Rep. Tokoku Univ. Ser. III,* **6,** 261–310.
Bailey, D. K. (1969) *Am. J. Sci.* **267-A,** 1–16.
——and Schairer, J. F. (1966) *J. Petrol.* **7,** 114–70.
Ernst, W. G. (1968) *Amphiboles.* Springer-Verlag, New York.
Ferguson, A. K. (1977*a*) *Contrib. Mineral. Petrol.* **60,** 247–53.
——(1977*b*) *Geol. Soc. Aust., J.* **24,** 491–4.
——(1978) *Contrib. Mineral. Petrol.* **67,** 11–15.
Flower, M. F. J. (1974) *Am. Mineral.* **59,** 536–48.
Frey, F. A., Green, D. H., and Roy, S. D. (1978) *J. Petrol.* **19,** 463–513.
Haggerty, S. E. (1976) In *Mineralogical Society of America short course notes,* **3** (Rumble D., III, ed.) Southern Printing Co., Blacksburg, Va., Hg 101–69.
Kogarko, L. N., and Krigman, L. D. (1973) *Geokhimiya* **1,** 49–56.
Larsen, L. M. (1976) *J. Petrol.* **17,** 258–90.
Nielsen, T. D. F. (1979) *Contrib. Mineral. Petrol.* **69,** 235–44.
Pedersen, A. K., Engell, J., and Rønsbo, J. G. (1975) *Lithos,* **8,** 255–68.
Rønsbo, J. G., Pedersen, A. K., and Engell, J. (1977) Ibid. **10,** 193–204.
Scott, P. W. (1976) *Mineral. Mag.* **40,** 805–16.
Yagi, K. (1953) *Geol. Soc. Am. Bull.* **64,** 769–810.